Analysis and Calculation of Zero-Sequence Voltage Considering Neutral-Point Potential Balancing in Three-Level NPC Converters

Chenchen Wang, *Member, IEEE*, and Yongdong Li

***Abstract*—The neutral-point (NP) potential of the three-level neutral-point-clamped converters is needed to maintain balancing. Zero-sequence voltage is the only freedom degree when carrier-based pulsewidth modulation is utilized. Appropriate zero-sequence voltage should be identified to control the NP potential. The relationship between the neutral current and injected zero-sequence voltage is studied comprehensively, and two balancing algorithms of NP potential, respectively adopting searching-optimization and interpolation methods, are presented. The theoretical optimum zero-sequence voltage for controlling NP potential can be obtained by the latter proposed algorithm. Simulation and experimental results are shown to verify the validity and practicability of the proposed algorithms.**

***Index Terms*—Balancing algorithm, neutral point clamped (NPC), neutral-point (NP) potential, zero-sequence voltage.**

I. Introduction

THREE-LEVEL neutral-point-clamped (NPC) converters [1] have been widely applied in the medium-voltage power conversion [2]–[4]. One of the essential problems of the NPC converters is that how to keep the voltage of dc-link capacitors balancing, in other words, keep the neutral-point (NP) potential stable and suppress the ripple [5]. If the NP potential is not controlled effectively, the output voltage of the converter would deviate from the reference value; moreover, the devices and equipment might be damaged.

The control strategies of NP potential that have appeared in the literatures can be summarized according to the pulsewidth modulation (PWM) algorithm utilized. If space-vector PWM (SVPWM) is used, the voltage vectors can be classified into four categories by their magnitude: zero vectors, small vectors, middle vectors, and large vectors. Then, the relationship between NP potential and each switching state vector can be analyzed. It is known that the zero vectors and large vectors have no effect on NP potential, but the middle vectors and small vectors have effect on it. It is noticed that there are two switching states (positive and negative) that have reverse action (charging or discharging) on NP potential for one small vector. Therefore, the main task is to adjust the dwell time between the duplicate switching states of small vectors [6]–[10].

Correspondingly, if carrier-based PWM (CPWM) is used, the control of the NP potential can be considered as the problem of identifying the zero-sequence voltage. The zero-sequence voltage injected into the reference voltages does not change the output line voltages, but influences the switching states and of course the NP potential. The NP potential variation caused by the injected zero-sequence voltage was studied, and some algorithms to keep the NP potential balancing by injecting the appropriate zero-sequence voltage were presented in [11]–[15]. The low-frequency voltage oscillations in the neutral point were also studied, and the solution was presented in [16]–[18]. However, higher switching frequency and extra switching losses of converter are unavoidable.

It is known that, the zero-sequence voltage is the only freedom degree which can be adjusted in the process of modulation. The relationship between SVPWM and CPWM has been studied, and the identity of them has been obtained [19], [20]. Essentially, selecting redundant switching states and adjusting dwell time in SVPWM is the process of deciding the zero-sequence voltage. Therefore, the zero-sequence voltage should be taken focus on when the problem of NP potential balancing is considered. It is noticed that no matter which modulation method is adopted, the neutral current is an important variable. Once the neutral current is known, the NP potential variation can be obtained. On the other hand, once the zero-sequence voltage is identified, the switching state is determined. In addition, according to the three-phase currents and switching state, the neutral current can be calculated. However, the relationship between the neutral current and the zero-sequence voltage is not linear and continuous, which causes that the algorithm is not direct and facility.

The relationship between neutral current and injected zero-sequence voltage in three-level NPC converters is studied in this paper comprehensively. A searching-optimization algorithm to balance the NP potential is presented, and an interpolation method to calculate the exact zero-sequence voltage for NP potential balancing is proposed simultaneously, which is called precise calculation algorithm in this paper. The two presented methods are verified through the simulation and experimental results.

Manuscript received February 1, 2009; revised April 19, 2009 and May 11, 2009; accepted May 15, 2009. Date of publication June 5, 2009; date of current version June 11, 2010.

C. Wang is with the School of Electrical Engineering, Beijing Jiaotong University, Beijing 100044, China (e-mail: chchwang@bjtu.edu.cn).

Y. Li is with the Department of Electrical Engineering, Tsinghua University, Beijing 100084, China (e-mail: liyd@mail.tsinghua.edu.cn).

Color versions of one or more of the figures in this paper are available online at http://ieeexplore.ieee.org.

Digital Object Identifier 10.1109/TIE.2009.2024093

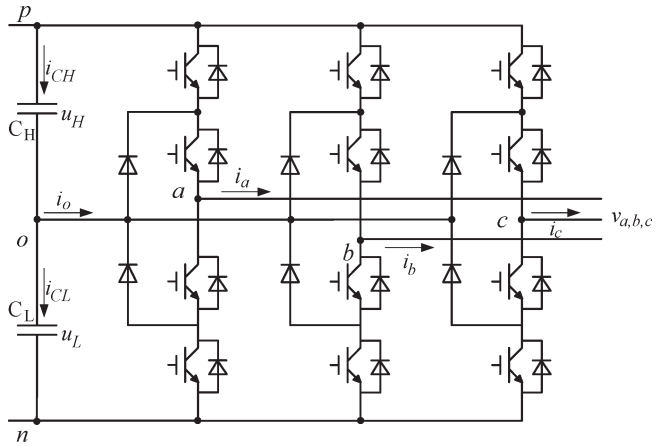

Fig. 1. Three-level NPC inverter.

II. Relationship Between Neutral Current and Zero-Sequence Voltage

Fig. 1 shows a schematic diagram of a three-level NPC inverter. In order to simplify the analysis, several assumptions are made here.

1) The dc-link voltage is constant. Then, the influence of the dc-link voltage on the NP potential can be eliminated.
2) The upper capacitor and the lower capacitor in the dc-link have the same capacitance and characteristic, i.e., $C_{\rm H} = C_{\rm L} = C$.
3) The inverter is connected to a three phase balanced load. The three-phase voltages and currents are purely sinusoidal and symmetrical.
4) The modulation frequency is higher enough than the output fundamental frequency, and the phase currents can be considered as constant in a modulation period.

If $V_{\rm dc}/2$ ($V_{\rm dc}$ is defined as the dc-link voltage) is selected as the base value, the three phase positive-sequence reference voltages can be normalized as

$$\begin{aligned} v_{a0} &= m \cdot (2/\sqrt{3}) \cdot \cos\theta \\ v_{b0} &= m \cdot (2/\sqrt{3}) \cdot \cos(\theta - 2\pi/3) \\ v_{c0} &= m \cdot (2/\sqrt{3}) \cdot \cos(\theta + 2\pi/3) \end{aligned} \tag{1}$$

where m is modulation index, and $0 \le m \le 1$; (The maximum modulation index can achieve one in linear modulation area by space vector modulation (SVM) or by carried-based PWM strategies that make use of proper zero-sequence voltage); θ is phase angle, and $\theta = \omega t$, where ω is the angular frequency.

If the zero-sequence voltage (v_0) is injected into the three phase reference voltages, the actual reference voltages can be given by

$$\begin{aligned} v_a &= v_{a0} + v_0 \\ v_b &= v_{b0} + v_0 \\ v_c &= v_{c0} + v_0. \end{aligned} \tag{2}$$

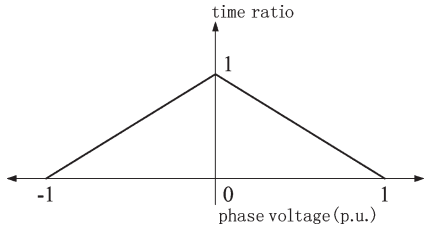

Fig. 2. Average phase voltage and time ratio of the neutral point output.

According to the aforementioned assumption, the three-phase currents of the converter can be given by

$$\begin{aligned} i_a &= I_m \cos(\theta - \varphi) \\ i_b &= I_m \cos(\theta - 2\pi/3 - \varphi) \\ i_c &= I_m \cos(\theta + 2\pi/3 - \varphi) \end{aligned} \tag{3}$$

where I_m is amplitude of the phase current and φ is power factor angle.

Generally, only a couple of devices switch on and off in a modulation period for a phase leg. For a three-level NPC converter, one-phase current makes contribution to the neutral current only when this phase is connected to the neutral point, that is to say, when this phase outputs zero-level voltage. Fig. 2 shows the relationship between an average phase voltage and a time ratio of the neutral point output [11]. Furthermore, it is known that in a three-leg three-wire system, $i_a + i_b + i_c = 0$. Therefore, the average neutral current in a modulation period can be obtained

$$i_o = \sum_{x=a,b,c} (1 - |v_x|) \cdot i_x = - \sum_{x=a,b,c} |v_x| \cdot i_x. \tag{4}$$

In addition, the NP potential variation can be easily calculated by the following equation:

$$\Delta u_{\rm L} = -\frac{1}{2C} \int i_{\rm o} dt. \tag{5}$$

For convenience of analysis, $v_{\max 0}/v_{\max}$, $v_{\rm mid0}/v_{\rm mid}$, $v_{\min 0}/v_{\min}$ are defined as the maximum, medium, minimum value of the reference voltages without/with injected zero-sequence voltage, and $i_{v\max}$, $i_{v\rm mid}$, $i_{v\min}$ as the current of the corresponding phase. The injected zero-sequence voltage will not modify the relation of magnitude, so

$$v_{\rm max,mid,min} = v_{\max 0,{\rm mid}0,\min 0} + v_0. \tag{6}$$

In this paper, the phase voltage is set as $-1 \le v_x \le 1$, $x \in [a, b, c]$, so the span of the zero-sequence voltage that can be injected is expressed as

$$v_{0\_\min} \le v_0 \le v_{0\_\max} \tag{7}$$

where

$$v_{0\_\min} = -1 - v_{\min 0} \quad v_{0\_\max} = 1 - v_{\max 0}$$

are, respectively, defined as the smallest and biggest zero-sequence voltages that can be injected.

In (4), it can be seen that the average neutral current is related with the phase currents and the absolute value of the reference voltages. It seems like that the zero-sequence voltage which can keep the NP potential balancing could be straightforward calculated. The only problem need to be resolved is the polarity of phase voltage. Reference [11] simply dealt with it by considering the polarity in different section and gave the zero-sequence voltage forcing the neutral current to be zero in Section I as

$$v_0 = \frac{m}{2}\frac{\frac{1}{2}\cos\theta + \cos(2\varphi - \theta)}{\sin(\varphi - \theta)}. \tag{8}$$

However, it is noted that the polarity of phase voltage added the zero-sequence voltage possibly reverses. Correctly, the injected zero-sequence voltage should be expressed as [13]

$$v_0 = \frac{-i_o - [S_{\mathrm{sgna}} \cdot v_{a0} \cdot i_a + S_{\mathrm{sgnb}} \cdot v_{b0} \cdot i_b + S_{\mathrm{sgnc}} \cdot v_{c0} \cdot i_c]}{S_{\mathrm{sgna}} \cdot i_a + S_{\mathrm{sgnb}} \cdot i_b + S_{\mathrm{sgnc}} \cdot i_c} \tag{9}$$

where i_o which can be obtained in terms of (9) is the expected neutral current that keep the NP potential balancing. It is attended that here

$$[S_{\mathrm{sgna}}, S_{\mathrm{sgnb}}, S_{\mathrm{sgnc}}]^{\mathrm{T}} = [\mathrm{sgn}(v_a), \mathrm{sgn}(v_b), \mathrm{sgn}(v_c)]^{\mathrm{T}}.$$

Unfortunately, $\mathrm{sgn}(v_x)$ is not certain when different zero-sequence voltages are injected. In order to solve this problem, a test-verify-revise algorithm for NP potential balancing was presented in [13]. First, the polarity of phase voltage with injected zero-sequence voltage was assumed to be the same as the polarity of positive-sequence voltage, then the prediction result $v_{0\mathrm{test}}$ should be substituted into (7) and the validity of the assumption on polarity was verified. If the result did not accord with the assumption, the sign of v_{mid} would be revised and substituted into (9) to obtain the new result. The change of the other phase voltage was not considered and the trouble of the polarity caused by injected zero-sequence voltage was settled indirectly.

III. Further Analysis and the Proposed NP Potential Balancing Algorithms

The most comprehensive method is to traverse all the zero-sequence voltages that can be injected, and choose the most helpful one for the NP potential balancing. However, it is not suitable for application. For simplicity, some important zero-sequence voltages are selected and compared. The parameter L and k were defined to represent the serial number of each switch sequence and the ratio of duration time between the duplicate voltage vector [21]–[23]. The zero-sequence voltages which can be easily obtained when $k = 0$ and $L = 0, 1, 2, \ldots$ (at least one-phase output voltage is integer level) can be selected and intercompared, then the most appropriate one will be chosen. This process is called searching-optimization strategy. It is shown in Fig. 3 that, for a three-level converter, there will be five zero-sequence voltages for comparison in the central meshed region, comparatively, three in the white region and two in the outside gray region. Obviously, the result is only a comparatively optimal one, but the computation is restricted. The practicality will be shown in the later section.

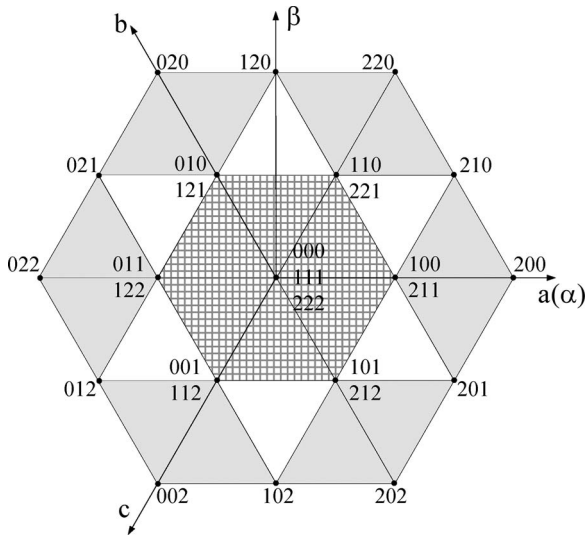

Fig. 3. Three-level space-vector diagram.

It is necessary to further analyze the relationship between the neutral current and zero-sequence voltage. For $v_{a0} + v_{b0} + v_{c0} = 0$, there must be $v_{\max 0} \geq 0$, $v_{\min 0} \leq 0$. Only the sign of $v_{\mathrm{mid}0}$ is not determined. However, whatever the sign is, the relationship between the neutral current and zero-sequence voltage v_0 can be derived as follows according to the value of v_0.

1) $v_0 \geq -v_{\min 0}$, then the three phase reference voltages are all nonnegative. The average neutral current is

$$\begin{aligned} i_o &= -v_{\max} \cdot i_{v\max} - v_{\mathrm{mid}} \cdot i_{v\mathrm{mid}} - v_{\min} \cdot i_{v\min} \\ &= -v_{\max 0} \cdot i_{v\max} - v_{\mathrm{mid}0} \cdot i_{v\mathrm{mid}} - v_{\min 0} \cdot i_{v\min} = i'_o. \end{aligned} \tag{10}$$

2) $-v_{\mathrm{mid}0} < v_0 < -v_{\min 0}$, then $v_{\min} \leq 0$, $v_{\mathrm{mid}} \geq 0$, $v_{\max} \geq 0$. The average neutral current is

$$\begin{aligned} i_o &= -v_{\max} \cdot i_{v\max} - v_{\mathrm{mid}} \cdot i_{v\mathrm{mid}} + v_{\min} \cdot i_{v\min} \\ &= -v_{\max 0} \cdot i_{v\max} - v_{\mathrm{mid}0} \cdot i_{v\mathrm{mid}} \\ &\quad + v_{\min 0} \cdot i_{v\min} + 2 \cdot i_{v\min} \cdot v_0. \end{aligned} \tag{11}$$

The span of average neutral current is denoted by i'_o and i''_o, which are the neutral currents when $v_0 = -v_{\min 0}$ and $v_0 = -v_{\mathrm{mid}0}$

$$i'_o = -v_{\max 0} \cdot i_{v\max} - v_{\mathrm{mid}0} \cdot i_{v\mathrm{mid}} - v_{\min 0} \cdot i_{v\min} \tag{12}$$

$$\begin{aligned} i''_o &= -v_{\max 0} \cdot i_{v\max} - v_{\mathrm{mid}0} \cdot i_{v\mathrm{mid}} + v_{\min 0} \cdot i_{v\min} \\ &\quad - 2 \cdot v_{\mathrm{mid}0} \cdot i_{v\min}. \end{aligned} \tag{13}$$

3) $-v_{\max 0} < v_0 \leq -v_{\mathrm{mid}0}$, then $v_{\min} \leq 0$, $v_{\mathrm{mid}} \leq 0$, $v_{\max} \geq 0$. The average neutral current is

$$\begin{aligned} i_o &= -v_{\max} \cdot i_{v\max} + v_{\mathrm{mid}} \cdot i_{v\mathrm{mid}} + v_{\min} \cdot i_{v\min} \\ &= -v_{\max 0} \cdot i_{v\max} + v_{\mathrm{mid}0} \cdot i_{v\mathrm{mid}} \\ &\quad + v_{\min 0} \cdot i_{v\min} - 2 \cdot i_{v\max} \cdot v_0. \end{aligned} \tag{14}$$

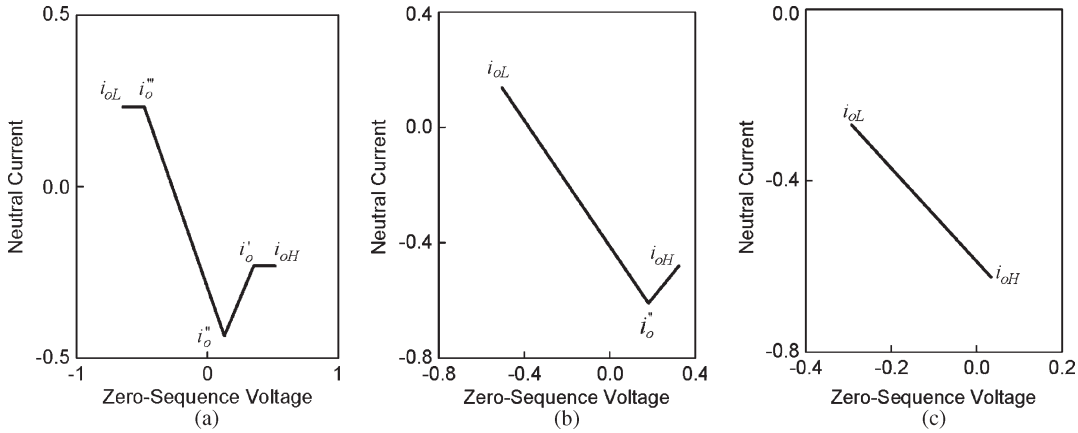

Fig. 4. Average neutral current (in per unit) caused by zero-sequence voltage. (a) Case 1. (b) Case 2. (c) Case 3.

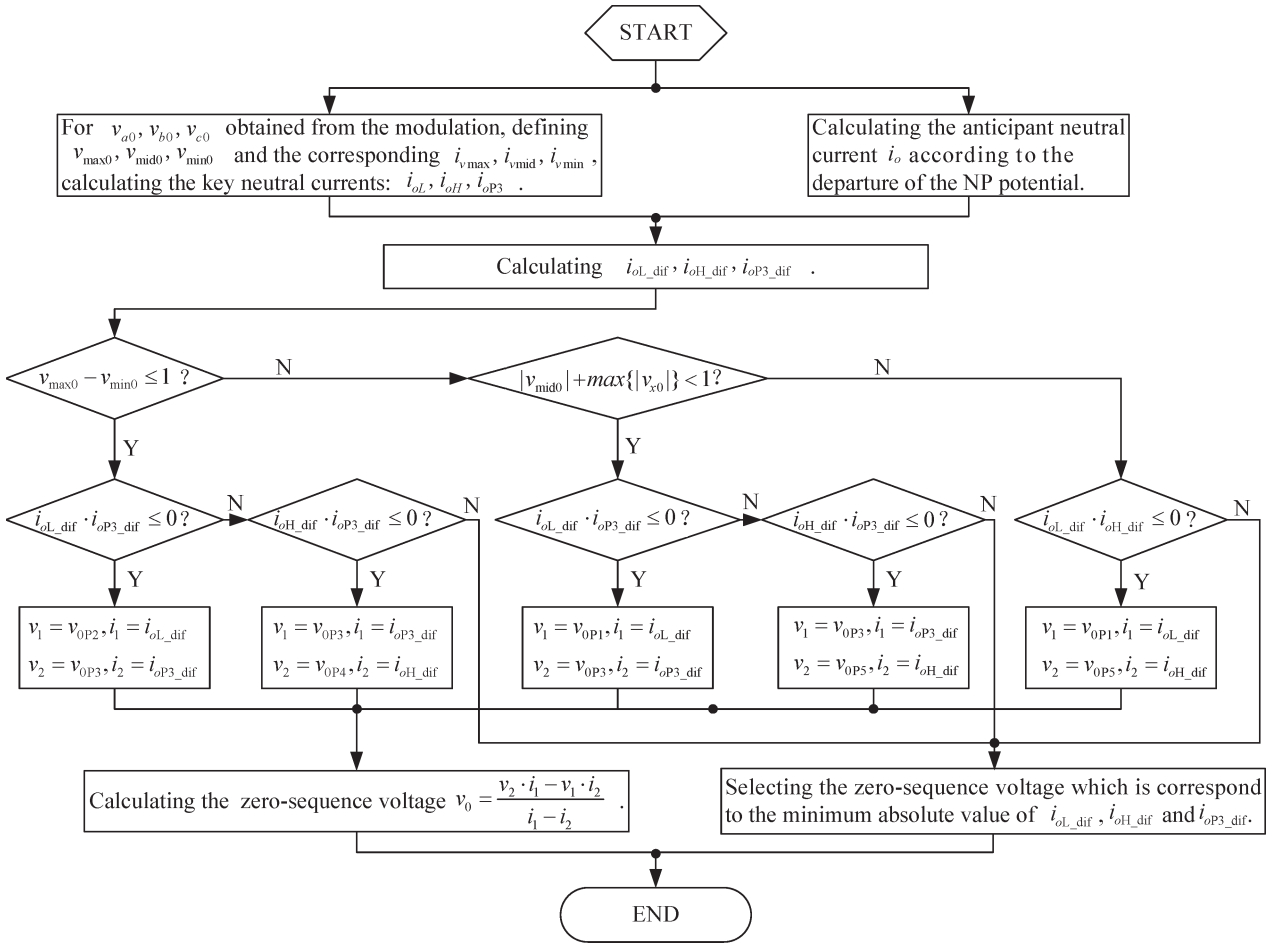

Fig. 5. Flowchart of the proposed algorithm.

The span of average neutral current is denoted by i_o'' and i_o''', where i_o''' is the neutral current when $v_0 = -v_{\max 0}$

$$i_o''' = v_{\max 0} \cdot i_{v\max} + v_{\mathrm{mid}0} \cdot i_{v\mathrm{mid}} + v_{\min 0} \cdot i_{v\min}. \quad (15)$$

4) $v_0 \le -v_{\max 0}$, then the reference voltages are all nonpositive. The average neutral current is

$$i_o = v_{\max 0} \cdot i_{v\max} + v_{\mathrm{mid}0} \cdot i_{v\mathrm{mid}} + v_{\min 0} \cdot i_{v\min} = i_o'''. \quad (16)$$

It is noticed that the possible neutral currents are expressed from (10)–(16). For different modulation index and phase angle, the four conditions discussed above might not exist simultaneously. According to the quantity of the reference voltages, it is not difficult to classify the all possible states to three cases.

Case 1) $v_{\max 0} - v_{\min 0} \le 1$

In this case, the reference voltages can be all nonpositive and nonnegative with injected zero-sequence voltage. The curve of neutral current

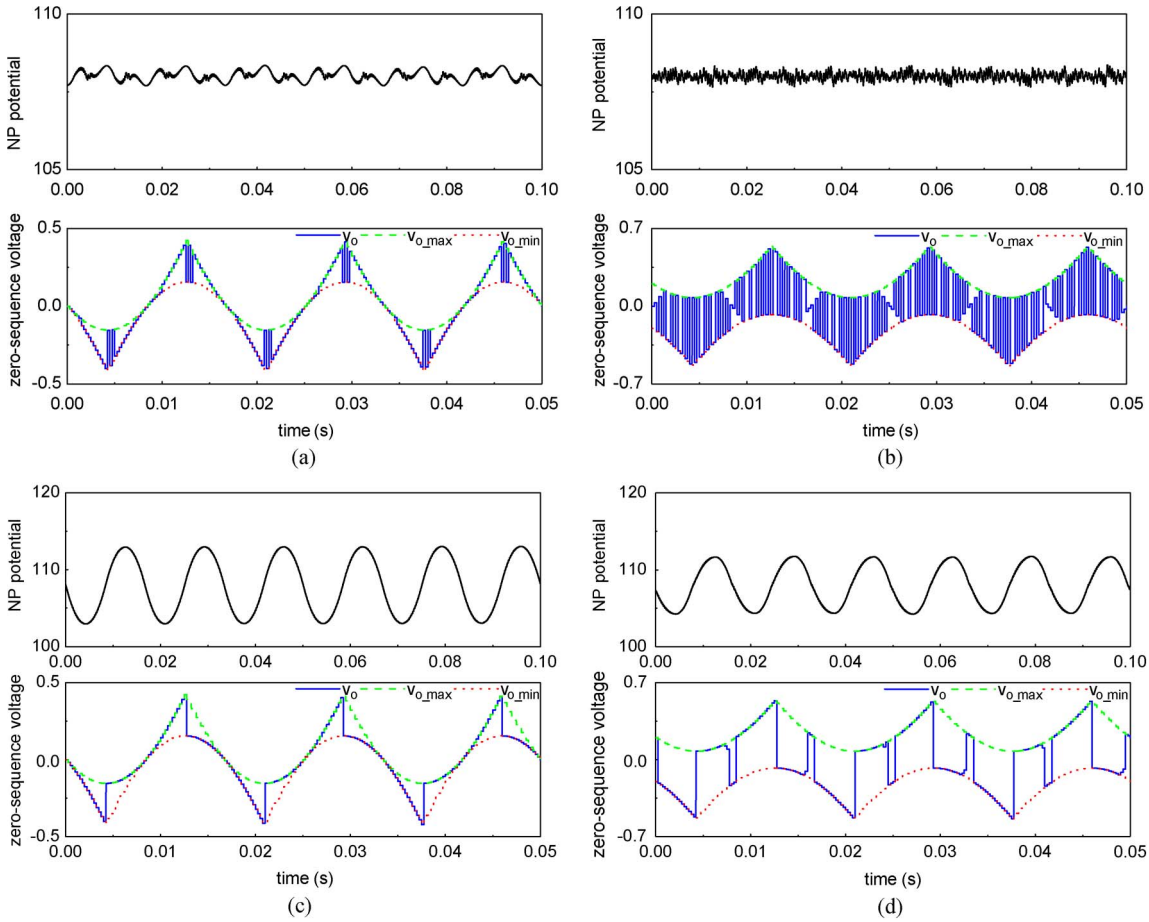

Fig. 6. NP potential and zero-sequence voltage with different modulation index and power factor, when the searching-optimization algorithm is used. (a) $m = 1$, $\varphi = 0$. (b) $m = 0.8$, $\varphi = 0$. (c) $m = 1$, $\varphi = \pi/2$. (d) $m = 0.8$, $\varphi = \pi/2$.

versus zero-sequence voltage is shown in Fig. 4(a). It can be seen that the curve is composed of two line segments which are linear with the zero-sequence voltage and two line segments which are not varied with it. Specially, i_{oL} and i_{oH} denote the average neutral currents when $v_0 = -1 - v_{\min 0}$ and $v_0 = 1 - v_{\max 0}$. Here, the four conditions of neutral current are all exist in this case, and $i_{oL} = i_o'''$, $i_{oH} = i_o'$.

Case 2) $v_{\max 0} - v_{\min 0} > 1$ and $|v_{\mathrm{mid}0}| + \max\{|v_{x0}|\} < 1$, where $\max\{|v_{x0}|\}$ is the maximum absolute values of the reference voltages.

In this case, the reference voltages cannot be all nonpositive and nonnegative ($m = 0$ is not considered), but v_{mid} can alter its polarity. As shown in Fig. 4(b), only two line segments linear with the zero-sequence voltage remain. i_o' and i_o''' cannot be acquired any more. Average neutral current is confined by i_{oL}, i_o'', and i_{oH}.

Case 3) $|v_{\mathrm{mid}0}| + \max\{|v_{x0}|\} \geq 1$.

In this case, the injected zero-sequence voltage cannot alter the polarity of any phase voltage. Only i_{oL} and i_{oH} can be obtained, and the curve of average neutral current versus zero-sequence voltage is a line segment, as shown in Fig. 4(c).

According to the aforementioned analysis, there are five significant points formed by the zero-sequence voltage and corresponding neutral current:

P1) $v_{0\mathrm{P}1} = -1 - v_{\min 0}$, $i_{o\mathrm{P}1} = i_{oL}$;
P2) $v_{0\mathrm{P}2} = -v_{\max 0}$, $i_{o\mathrm{P}2} = i_o'''$;
P3) $v_{0\mathrm{P}3} = -v_{\mathrm{mid}0}$, $i_{o\mathrm{P}3} = i_o''$;
P4) $v_{0\mathrm{P}4} = -v_{\min 0}$, $i_{o\mathrm{P}4} = i_o'$;
P5) $v_{0\mathrm{P}5} = 1 - v_{\max 0}$, $i_{o\mathrm{P}5} = i_{oH}$.

It is shown in Fig. 4 that all available average neutral current values would not exceed the maximum and minimum values of the aforementioned five points. For an expected neutral current i_o, it needs to determine which line segment the neutral current locates in firstly. For example, in case 1, because $i_o' = i_{oH}$, $i_o''' = i_{oL}$, it only needs to identify that which interval i_o is in, either between P2 and P3 or between P3 and P4. Once the interval between Px and Py is confirmed, it is easy to calculate the corresponding zero-sequence voltage using interpolation method as follows:

$$v_0 = \frac{v_{0\mathrm{Py}}(i_o - i_{o\mathrm{Px}}) - v_{0\mathrm{Px}}(i_o - i_{o\mathrm{Py}})}{i_{o\mathrm{Py}} - i_{o\mathrm{Px}}}. \tag{17}$$

Practically, the difference can be calculated

$$i_{o\mathrm{Px\_dif}} = i_o - i_{o\mathrm{Px}} \quad i_{o\mathrm{Py\_dif}} = i_o - i_{o\mathrm{Py}}. \tag{18}$$

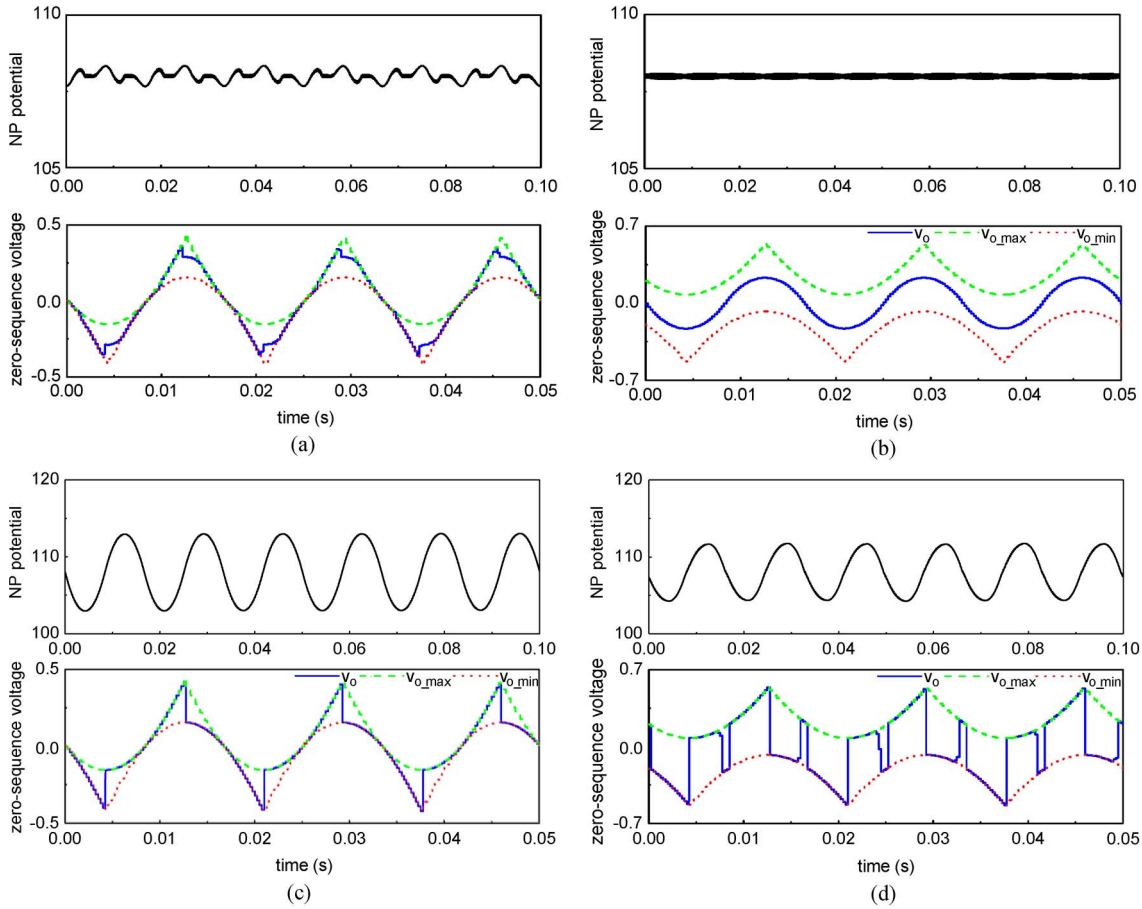

Fig. 7. NP potential and zero-sequence voltage with different modulation index and power factor, when precise calculation algorithm is used. (a) $m = 1, \varphi = 0$. (b) $m = 0.8, \varphi = 0$. (c) $m = 1, \varphi = \pi/2$. (d) $m = 0.8, \varphi = \pi/2$.

If $i_{o\mathrm{Px\_dif}} \cdot i_{o\mathrm{Py\_dif}} \leq 0$, then it can be confirmed that i_o locates in the interval between Px and Py, and the corresponding zero-sequence voltage is

$$v_0 = \frac{v_{0\mathrm{py}} \cdot i_{o\mathrm{Px\_dif}} - v_{0\mathrm{px}} \cdot i_{o\mathrm{Py\_dif}}}{i_{o\mathrm{Px\_dif}} - i_{o\mathrm{Py\_dif}}}. \tag{19}$$

For simply description, we call this strategy precise calculation algorithm. It is noted that, i_o may locate in two line segments simultaneously in case 1 and case 2. Both results are acceptable. Of course, i_o also may locate in none of the line segments. At this time, the neutral current which is most closed to the expected neutral current will be selected. $i_{o\mathrm{P1\_dif}}$, $i_{o\mathrm{P5\_dif}}$, and $i_{o\mathrm{P3\_dif}}$ (if P3 is available) are calculated, and the one that has the minimum absolute value can be considered as the optimum solution. Fig. 5 shows the flowchart of the proposed algorithm. The exact zero-sequence voltage that is thought as the most optimal for NP potential balancing can be gained exactly and conveniently.

IV. Simulation and Experimental Results

In this section, some simulation results will be given to verify the proposed method. The parameters that used in simulation are listed as follows: $V_{\mathrm{dc}} = 216$ V, $I_{\mathrm{Load}}(rms) = 2.5$ A, $C = 740$ μF, $f_{\mathrm{sw}} = 4$ kHz, $f = 20$ Hz.

The elements that have effect on the NP potential fluctuation have been studied, and the main conclusion is as follows: Besides the capacitance of dc capacitor, load current, and the length of the control period, the modulation index and the power factor can also influence the NP potential ripple; the NP potential fluctuation will be severer when the modulation index is closer to one, and the power factor angle is closer to $\pm\pi/2$ [7], [24], [25]. Figs. 6 and 7 show the NP potential when the searching-optimization and the precise calculation algorithm are used. Two typical power factors (power factor angle $\varphi = 0$ and $\pi/2$) are considered. Furthermore, two modulation indexes ($m = 1$ and 0.8) are selected for analysis because the fluctuation of NP potential is not obvious when modulation index is small. The injected zero-sequence voltages obtained by the corresponding methods are also shown in the simulation results. The maximum and the minimum zero-sequence voltage [see (7)] that can be injected are given simultaneously. Obviously, the NP potential can be maintained steady whichever algorithm is used, even though the ripple is in evidence when $\varphi = \pi/2$.

It is noticed that, when the fluctuation of NP potential is severe, such as the modulation index is large $(m = 1)$ or the power factor is low $(\varphi = \pi/2)$, the injected zero-sequence voltages calculated by the two algorithms are nearly the same. It can be thought that in this instance, the control margin of NP potential is small, so generally the maximum or the

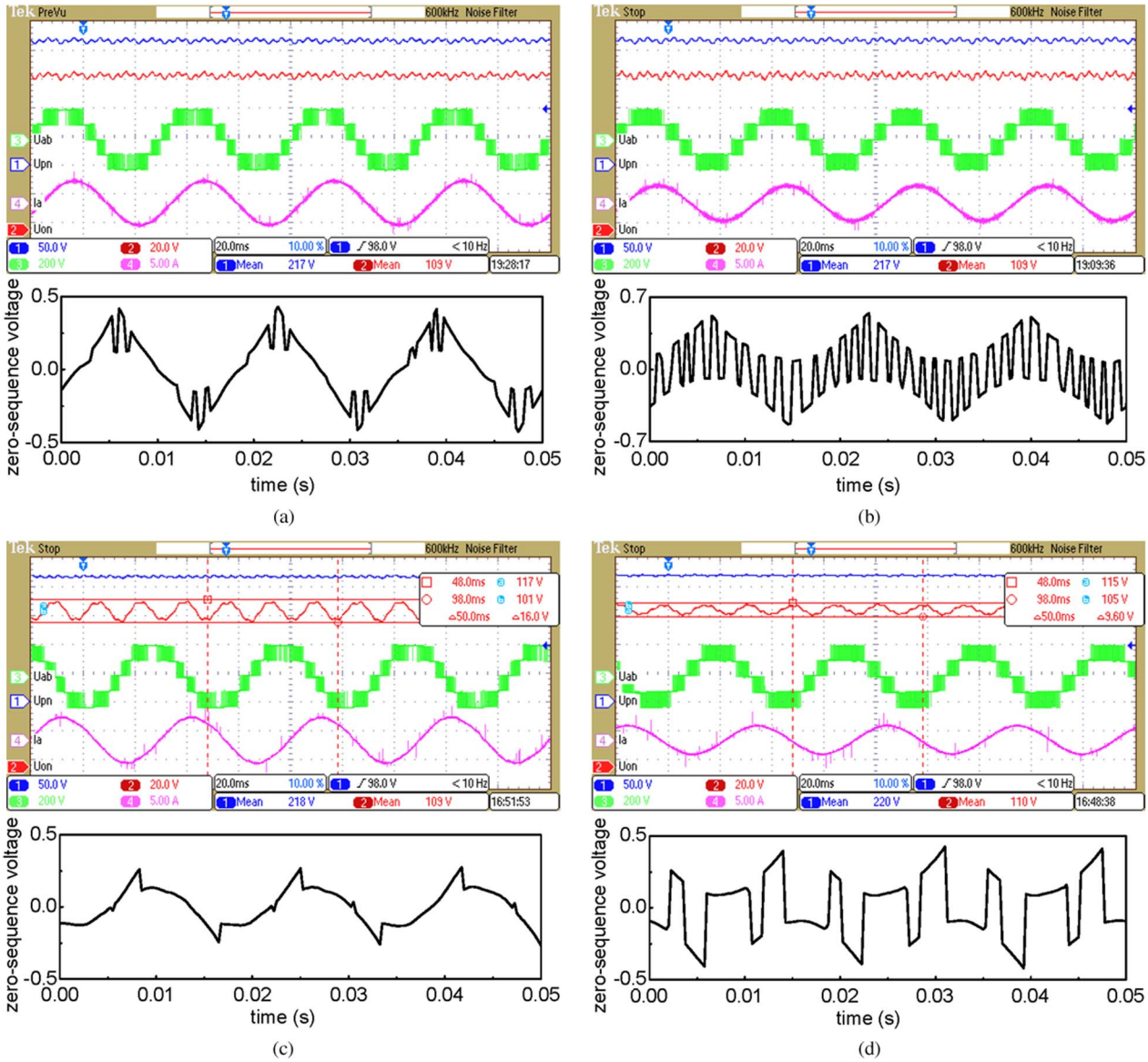

Fig. 8. Experimental results when the searching-optimization algorithm is used. (a) R–L load, $M = 1.0$. (b) R–L load, $M = 0.8$. (c) IM load, $M = 1.0$. (d) IM load, $M = 0.8$. (The converter operates at 20 Hz with R–L load or IM load. For each illustration, respectively, (blue) dc-link voltage, (red) NP potential, (green) line voltage of converter, (pink) line current of the converter, and the (black) injected zero-sequence voltage are shown from the top down.)

minimum zero-sequence voltage will be selected as the injected one. It is evident in Figs. 6(a), (c), and (d) and 7(a), (c), and (d). Otherwise, the precise calculation algorithm can obtain the more precise result than the searching-optimization one, which can be compared in Figs. 6(b) and 7(b). Nevertheless, in this instance, the fluctuation of NP potential is small, and the improvement of the precise calculation algorithm is not significant. However, it cannot be denied that the precise calculation algorithm is the more accurate one.

The presented algorithms are also validated by experiments. A CM15YE13-12H IPM is used to build the little three-level NPC inverter. The capacitor in dc-link is 740 μF, and the dc-link voltage is approximately set to 216 V. TMS320F2812 is used as the main controller. Two operating states are considered. One is that a three phase load consisting of inductance (4.2 mH) and resistance (31.3 Ω) is connected to the inverter. The power factor is 0.9999 theoretically when the converter operates at 20 Hz with the R–L wye-connected load, representing the condition of high power factor. The other one is that the inverter feeds an induction motor (IM) with no load. The parameters of the IM are the following: 2.2 kW, 380 V, 5 A, 50 Hz. Because the dc-link voltage of inverter is approximately set to 216 V, when the no-load motor operates at 20 Hz with rated flux, the modulation index is about unit, and the power factor is about 0.085, representing the condition of low power factor.

Figs. 8 and 9 show the experimental results when the searching-optimization algorithm and the precise calculation algorithm are utilized. Similar with the simulation results, the NP potential ripple is suppressed satisfactorily except at high-modulation index, low power factor. For a passive front is used, the variation of the dc-link voltage cannot be neglected. Under the experimental condition previously mentioned, if the inverter operates in high power factor, the fluctuation of NP

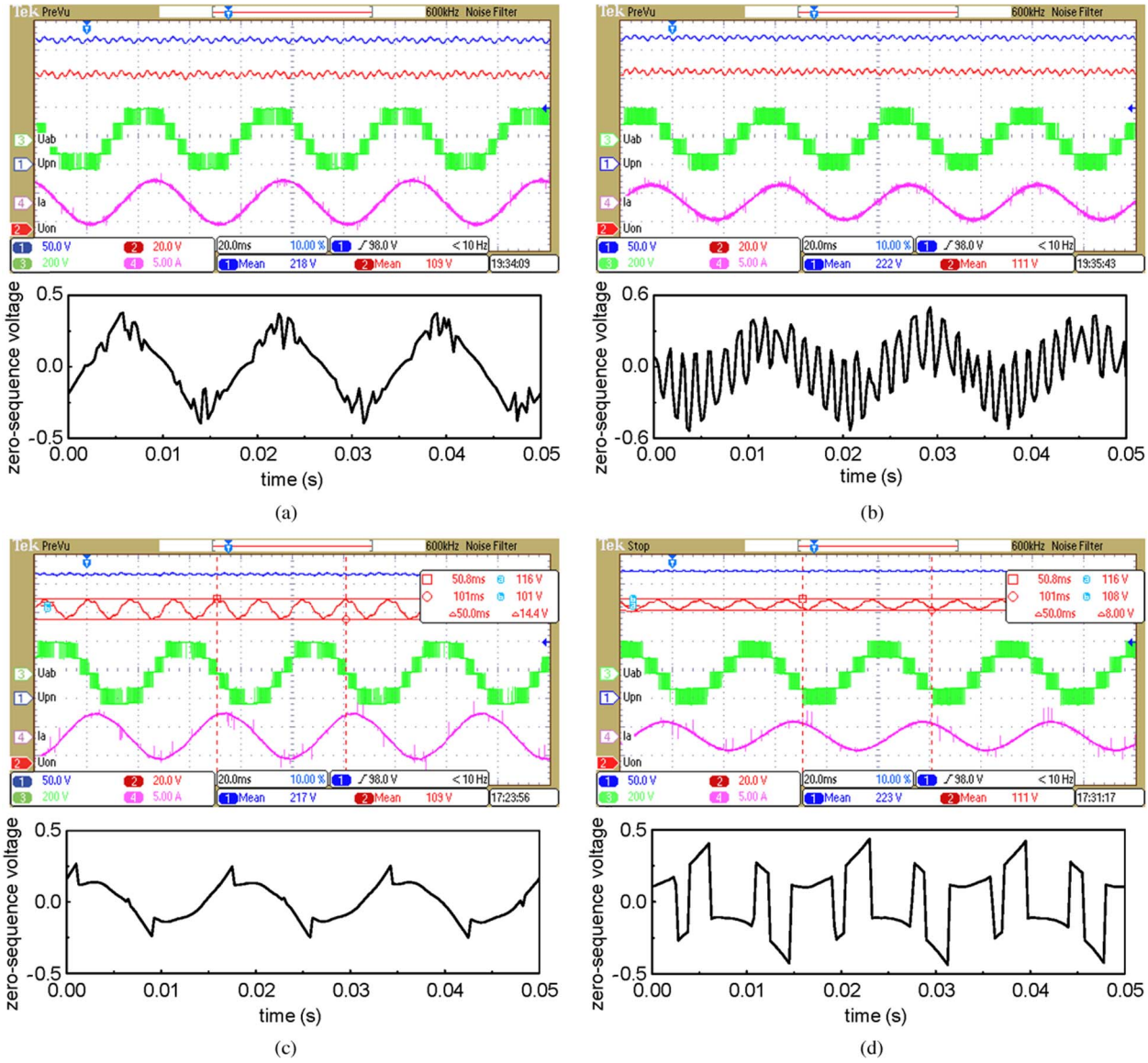

Fig. 9. Experimental results when the precise calculation algorithm is used. (a) R–L load, $M = 1.0$. (b) R–L load, $M = 0.8$. (c) IM load, $M = 1.0$ (d) IM load, $M = 0.8$. (The converter operates at 20 Hz with R–L load or IM load. For each illustration, respectively, (blue) dc-link voltage, (red) NP potential, (green) line voltage of converter, (pink) line current of the converter, and the (black) injected zero-sequence voltage are shown from the top down.)

potential is inconspicuous, comparing with the fluctuation of dc-link voltage. The peak-to-peak value of the NP potential fluctuation is also measured when the inverter operates in low power factor. Slight improvement when the precise calculation algorithm is used can be seen from the corresponding figures. Considering the nonideal factor in measurement, the improvement cannot be thought as the convincing argument.

Not only the stable but also the dynamic instances are considered. As shown in Fig. 10, the NP potential is controlled on one third of the dc-link voltage by the presented algorithm. Then, a command is given to the controller, and the NP potential is controlled to one half of the dc-link voltage rapidly, shorter than two operating periods.

Although the precise calculation algorithm is much better than the searching-optimization one through the theoretical analysis, the advantage is not exhibited evidently in the simulation and experimental results. Aside from the reason referred to when the simulation results are analyzed, there may be some other assignable causes, such as measuring and numerical errors, delay of the digital control, inaccuracy of the parameters, etc. It also can be seen that the injected zero-sequence voltages shown in Figs. 8 and 9 are not identical with the simulation results in Figs. 6 and 7. Therefore, the two presented algorithms are both good choices, for there may not be obvious distinctions in the control performance of NP potential between them. However, the precise calculation algorithm is the proposed one by the author.

Furthermore, the comprehensive analysis of the relationship between the neutral current and zero-sequence voltage can be used to study the NP-fully controlled region [13]. The concept has been presented in [7], in which it was also called ripple-free area. In order to achieve the so-called fully controlled region for one modulation index and one power factor, the neutral current must be kept zero. According to the proposed algorithm, the acquired region is shown in Fig. 11, which is most similar to

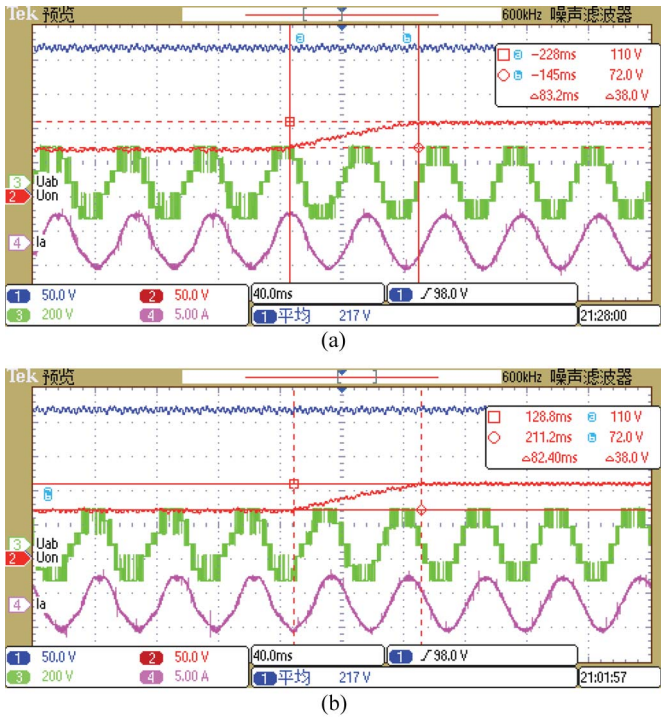

Fig. 10. NP potential is controlled from one third to half of the dc-link voltage. (a) Searching-optimization algorithm. (b) Precise calculation algorithm.

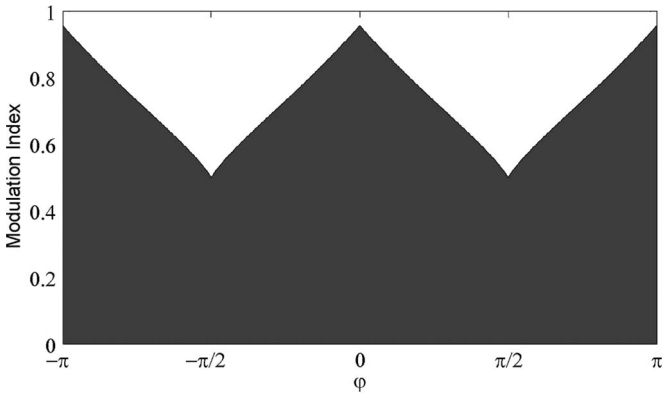

Fig. 11. NP-fully controlled region.

the one shown in [13] but has little difference with the one shown in [7]. Similarly, the normalized NP potential ripple is shown in Fig. 12, which is defined as (20) similar to that defined in [24]

$$\Delta v = \frac{\Delta u}{I_{\rm rms}/fC}. \tag{20}$$

V. Conclusion

A focus in the research of the three-level NPC converter, problem of NP potential balancing is studied comprehensively in this paper. For the relationship between the neutral current and the injected zero-sequence voltage is not linear and continuous, a detailed and deep discussion is necessary. Thanks for the achievement that has been acquired and presented in literatures, the relationship is further analyzed in this paper and made more clearly. Based on that, a searching-optimization

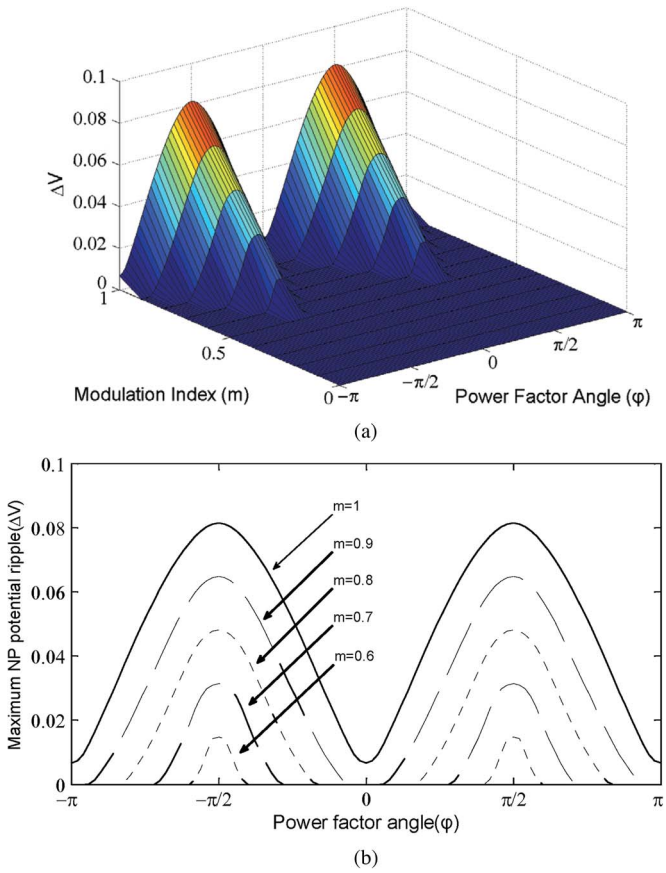

Fig. 12. Normalized amplitude of the NP potential ripple.

algorithm and a theoretical optimum algorithm employing interpolation method to precisely calculate the most appropriate zero-sequence voltage to control the NP potential are presented. Simulation and experiments are shown to verify the validity and the practicability of the proposed algorithms. Comparatively, the precise calculation algorithm that is based on the thorough and mathematical analysis of the relationship between the neutral current and zero-sequence voltage, is more superior and valuable, particularly in theory. The two presented algorithms both show the excellent performance in controlling NP potential of three-level NPC converters.

References

[1] A. Nabae, I. Takahashi, and H. Akagi, "A new neutral-point-clamped PWM inverter," *IEEE Trans. Ind. Appl.*, vol. IA-17, no. 5, pp. 518–523, Sep./Oct. 1981.

[2] G. Abad, M. A. Rodriguez, and J. Poza, "Three-level NPC converter-based predictive direct power control of the doubly fed induction machine at low constant switching frequency," *IEEE Trans. Ind. Electron.*, vol. 55, no. 12, pp. 4417–4429, Dec. 2008.

[3] M. Malinowski, S. Stynski, W. Kolomyjski, and M. P. Kazmierkowski, "Control of three-level PWM converter applied to variable-speed-type turbines," *IEEE Trans. Ind. Electron.*, vol. 56, no. 1, pp. 69–77, Jan. 2009.

[4] J. D. Barros and J. F. Silva, "Optimal predictive control of three-phase NPC multilevel converter for power quality applications," *IEEE Trans. Ind. Electron.*, vol. 55, no. 10, pp. 3670–3681, Oct. 2008.

[5] J. Rodriguez, S. Bernet, W. Bin, J. O. Pontt, and S. Kouro, "Multilevel voltage-source-converter topologies for industrial medium-voltage drives," *IEEE Trans. Ind. Electron.*, vol. 54, no. 6, pp. 2930–2945, Dec. 2007.

[6] W. Lixiang, W. Yuliang, L. Chongjian, W. Huiqing, L. Shixiang, and L. Fahai, "A novel space vector control of three-level PWM converter," in *Proc. IEEE Power Electron. Drive Syst.*, 1999, pp. 745–750.

[7] N. Celanovic and D. Boroyevich, "A comprehensive study of neutral-point voltage balancing problem in three-level neutral-point-clamped voltage source PWM inverters," *IEEE Trans. Power Electron.*, vol. 15, no. 2, pp. 242–249, Mar. 2000.
[8] K. Yamanaka, A. M. Hava, H. Kirino, Y. Tanaka, N. Koga, and T. Kume, "A novel neutral point potential stabilization technique using the information of output current polarities and voltage vector," in *Conf. Rec. IEEE IAS Annu. Meeting*, 2001, pp. 851–858.
[9] S. Busquets-Monge, J. D. Ortega, J. Bordonau, J. A. Beristain, and J. Rocabert, "Closed-loop control of a three-phase neutral-point-clamped inverter using an optimized virtual-vector-based pulsewidth modulation," *IEEE Trans. Ind. Electron.*, vol. 55, no. 5, pp. 2061–2071, May 2008.
[10] B. Abdul Rahiman, G. Narayanan, and V. T. Ranganathan, "Modified SVPWM algorithm for three level VSI with synchronized and symmetrical waveforms," *IEEE Trans. Ind. Electron.*, vol. 54, no. 1, pp. 486–494, Feb. 2007.
[11] S. Ogasawara and H. Akagi, "Analysis of variation of neutral point potential in neutral-point-clamped voltage source PWM inverters," in *Conf. Rec. IEEE IAS Annu. Meeting*, 1993, pp. 965–970.
[12] C. Newton and M. Sumner, "Neutral point control for multi-level inverters: Theory, design and operational limitations," in *Conf. Rec. IEEE IAS Annu. Meeting*, 1997, pp. 1336–1343.
[13] S. Qiang, L. Wenhua, Y. Qingguang, X. Xiaorong, and W. Zhonghong, "A neutral-point potential balancing algorithm for three-level NPC inverters using analytically injected zero-sequence voltage," in *Proc. IEEE Appl. Power. Electron. Conf.*, 2003, pp. 228–233.
[14] L. Jun, Q. H. Alex, Q. Zhaoming, and Z. Huijie, "A novel carrier-based PWM method for 3-level NPC inverter utilizing control freedom degree," in *Proc. IEEE Power Electron. Spec. Conf.*, 2007, pp. 1899–1904.
[15] A. Videt, P. Le Moigne, N. Idir, P. Baudesson, and X. Cimetiere, "A new carrier-based PWM providing common-mode-current reduction and dc-bus balancing for three-level inverters," *IEEE Trans. Ind. Electron.*, vol. 54, no. 6, pp. 3001–3011, Dec. 2007.
[16] J. Pou, J. Zaragoza, P. Rodriguez, S. Ceballos, V. M. Sala, R. P. Burgos, and D. Boroyevich, "Fast-processing modulation strategy for the neutral-point-clamped converter with total elimination of low-frequency voltage oscillations in the neutral point," *IEEE Trans. Ind. Electron.*, vol. 54, no. 4, pp. 2288–2294, Aug. 2007.
[17] J. Zaragoza, J. Pou, S. Ceballos, E. Robles, P. Ibaez, and J. L. Villate, "A comprehensive study of a hybrid modulation technique for the neutral-point-clamped converter," *IEEE Trans. Ind. Electron.*, vol. 56, no. 2, pp. 294–304, Feb. 2009.
[18] J. Zaragoza, J. Pou, S. Ceballos, E. Robles, C. Jaen, and M. Corbalan, "Voltage-balance compensator for a carrier-based modulation in the neutral-point-clamped converter," *IEEE Trans. Ind. Electron.*, vol. 56, pp. 305–314, Feb. 2009.
[19] V. Blasko, "Analysis of a hybrid PWM based on modified space-vector and triangle-comparison methods," *IEEE Trans. Ind. Appl.*, vol. 33, no. 3, pp. 756–764, May/Jun. 1997.
[20] W. Fei, "Sine-triangle versus space-vector modulation for three-level PWM voltage-source inverters," *IEEE Trans. Ind. Appl.*, vol. 38, no. 2, pp. 500–506, Mar./Apr. 2002.
[21] H. Xuan, L. Yongdong, and L. Yongheng, "A novel general space vector modulation algorithm for multilevel inverter based on imaginary coordination," in *Proc. IEEE Power Electron. Drive Syst.*, 2003, pp. 392–396.
[22] L. Yongdong, G. Yue, and H. Xuan, "A general SVM algorithm for multilevel converters considering zero-sequence component control," in *Proc. IEEE IECON*, 2005, pp. 508–513.
[23] C. Wang, Y. Li, and X. Xiao, "A unified SVM algorithm for multilevel converter and analysis of zero sequence voltage components," in *Proc. IEEE IECON*, 2006, pp. 2020–2024.
[24] J. Pou, R. Pindado, D. Boroyevich, and P. Rodriguez, "Evaluation of the low-frequency neutral-point voltage oscillations in the three-level inverter," *IEEE Trans. Ind. Electron.*, vol. 52, no. 6, pp. 1582–1588, Dec. 2005.
[25] C. Wang, "Research on the topology, PWM algorithm and balance control of neutral point voltage in multilevel converters," Ph.D. dissertation, Tsinghua Univ., Beijing, China, 2008.

Chenchen Wang (M'09) was born in Anhui Province, China, in 1981. He received the B.S. and Ph.D. degrees in electrical engineering from Tsinghua University, Beijing, China, in 2003 and 2008, respectively.

He is currently an Instructor with School of Electrical Engineering, Beijing Jiaotong University, Beijing. His research interests are multilevel converters and motor control.

Yongdong Li was born in Hebei Province, China, in 1962. He received the B.S. degree in electrical engineering from Harbin Institute of Technology, Harbin, China, in 1982 and the M.S. and Ph.D. degrees in electrical engineering from the Institut National Polytechnique de Toulouse, Toulouse, France, in 1984 and 1987, respectively.

He was a Postdoctoral Researcher from 1988 to 1990 and an Associate Professor from 1991 to 1996 with the Department of Electrical Engineering, Tsinghua University, Beijing, China. Since 1996, he has been a Professor with the same department of Tsinghua University. He is currently responsible of Laboratory of Power Electronics and Motor Control, Tsinghua University. His main interests include control theories, sensorless drives, and applications of ac motors; high-voltage, high-power inverter for motor drives, active power filter application, etc.

Dr. Li is a Senior Member of the China Electrotechnique Society, Vice Chairman of China Power Electronics Society, and Vice Chairman of Electrical Automation Committee of China Automation Association.